ARTICLE TYPE

Cite this: DOI: 00.0000/xxxxxxxxxx

Halogen-Copper Redox Chemistry as a Driving Force for Spherical Janus Microswimmers†

Kelly Henze,[a] Zuyao Xiao,[a] Khalifa Mohamed[b] and Juliane Simmchen*[b]

1 Methods

All chemicals that are used were purchased from Merck KGaA. The SiO_2 microspheres, the base for Janus particles, were purchased in different sizes of 2, 3, and 5 µm. To coat one hemisphere of the SiO_2 particles, copper (Cu, powder (dendritic), <45 µm, 99.7 % trace metals basis) is used. For the fuel bromine (Br_2, for analysis EMSURE® ACS, ISO, Reag. Ph Eur) and iodine (I_2, 99.99 % trace metals basis) are used. MilliQ water is used in all processes. The 24x24-sized glass slides of VWR International, LLC are used to prepare monolayers and microscopy.

1.1 Preparation of Cu@SiO_2 microswimmers

To generate Cu@SiO_2 particles, a suspension of the respective SiO_2 particles in MeOH is prepared. Followed by, 20 µl of the suspension is drop casted on a plasma-cleaned glass slide and set for drying in air. Once the monolayers are dried, they are coated by a thermal deposition device by Malz & Schmidt with the respective layer size (5 nm, 30 nm, or 50 nm) with a slow deposition rate. Afterward, a part of the coated monolayer is taken and dispersed in water by sonication for around 5 minutes to release the formed Janus particles. The last step is always done freshly before velocity measurements to ensure no oxidation started already.

1.2 Velocity experiments

The freshly suspended Cu@SiO_2 Janus particles are analyzed by their velocity with an Axio Observer optical microscope from Carl Zeiss Microscopy GmbH. All videos are recorded with an Axiocam 702 Mono from the same company with a frame rate of 40 fps and a 63x objective. The glass slides were first cleaned with EtOH and sonicated to use as a substrate for the microscopy, and then plasma cleaned. The reaction area is determined using the imaging spacers from Grace Bio-Lab's SecureSeal. For each reaction, 5 µl of the particle suspension is placed in a reaction area followed by 5 µl of the fuel, where in total, five different final concentrations are tested for bromine and iodine (10 µM, 25 µM, 50 µM, 100 µM, and 150 µM). The tracking starts directly after the addition of the fuel. For tracking, velocity, and MSD calculation, Matlab R2022a software with a code provided by Martin Wittmann from the TU Dresden is used. The code is tracking the particles' location and calculates the velocity using the change of position over the change of time. The mean velocity at different concentrations is then calculated as an average velocity of each tracked particle in the first 300 frames to ensure that velocity decreases are not taken into account due to the consumption of the provided fuel. Particles attached to the substrate glass are not considered for tracking and calculations. Additionally, the squared displacement is determined by measuring the difference between two positions across different time steps and squaring that value. Following the averages of these squared displacements across all available time intervals determines the mean squared displacement. To determine the impact of background ions like KCl, microscopy is conducted following the previous procedure. However, different concentrations of KCl solution are added to the Janus particle suspension initially to achieve final KCl concentrations of 10 µM, 100 µM, and 1000 µM in the microscopy solution.

1.3 Scanning electron microscopy and energy dispersive x-ray spectroscopy

For the SEM and EDX measurements, 100 µl of a prepared Janus Particle suspension is placed in a 1.5 ml Eppendorf tube, and 100 µl of the assigned fuel is added. The mixture was shaken for several seconds and left to react for 1 h. Afterward, the particles are washed once with water, and 2µl of each sample is placed on a sample holder and dried in air. The SEM measurements are taken with a Zeiss Gemini 300 instrument with an SE detector at 1.5 keV and a magnification of 15000x. The EDX measurements are done with the same device and an Ultim Max 65 detector from Oxford Instruments Nanoanalysis with 9 eV using the AZtec software from Oxford Instruments.

1.4 X-ray powder diffraction

To analyze the composition of the copper cap after the reaction with I_2, a sample is created by releasing the 5µm Cu@SiO_2 particles with a cap thickness of 50 nm from one complete glass slide (24 mm x 24 mm) into 1.5 ml water in a 2 ml Eppendorf tube. To make sure all of the particles are sedimented, the suspension is centrifuged for four minutes at 10000 rpm after the glass slides have been removed from the Eppendorf tube. Afterwards the supernatant is removed and 1.5 ml of 1 mM I_2 is added. The mixture was mixed for 10 s and left to react for 1 h. After this time the particles are centrifuged and 2 times washed with EtOH.

1.5 UV-VIS measurements

For the Cu^{2+} detection, a sample is generated by releasing the 5µm $Cu@SiO_2$ particles with a cap thickness of 50 nm from 1 whole glass slide into 1.5 ml water in a 2 ml Eppendorf tube. After removing the glass slides from the Eppendorf tube, the suspension is centrifuged for 4 min at 10000 rpm to ensure that all particles are sedimented. Afterward, 500 µl of the suspension was taken from the bottom of the Eppendorf tube and transferred to a 15 ml centrifuge tube. To ensure that the whole copper cap reacts with the bromine, 1 ml of a 1 mM bromine solution is added. The mixture is shaken for a few seconds and left to react for around 1h. Followed by an excess of 5 ml of NH_3 is added to the suspension and is shaken for a few seconds. In front of a white background, a slightly visible color change from transparent to light blue can be noticed by naked eye. As references, the Tetraammine-copper(II)-complex $[Cu(NH_3)_4]^{2+}$ is generated by $CuSO_4$ in different concentrations ($CuSO_4$, final concentrations: 10 mM, 1 mM, 0.1 mM, and 0.01 mM). The different solutions are analyzed using UV-Vis measurements from 400 to 800 nm with a Cary 60 UV-Vis spectrometer from Agilent Technologies, Inc.

1.6 pH measurements

A 24x24 glass slide layered with 30 nm of Cu was placed in 30 ml Br_2 solutions of different concentrations to monitor the pH value during the copper-bromine reaction. The pH was taken every minute during the reaction for 15 minutes at 20 ± 1 °C. As a reference, a 2 mM Br_2 solution was monitored without a copper slide.

1.7 Conductivity measurements

To record the conductivity values during the copper-bromine reaction, a 24x24 glass slide coated with a Cu(30 nm)@SiO_2(5µm) monolayer was immersed in 30 ml of Br_2 solutions of different concentrations. Conductivity measurements were taken every 15 seconds over a period of 3 minutes at a temperature of 17 ± 1 °C while the solution was stirred at 700 rpm.

1.8 Finite element simulation

To simulate the motion of $Cu@SiO_2$ particles in Br_2 and I_2 respectively, we developed a 2D axisymmetric model in COMSOL. The model consists of a 5 µm-diameter spherical particle placed at the center of a cylindrical computational domain with a diameter of 100 µm and a height of 100 µm. The cylinder is filled with water and serves as the calculation domain. Electric potential and fluid flow fields within this domain are simultaneously solved using a nonlinear steady-state solver in COMSOL. Since the particle is fixed in space and the fluid flows freely through the calculated domain, the particle's motion from the particle's own reference frame was modelled.

Three COMSOL modules were employed in this model: Transport of Diluted Species, Electrostatics and Creeping Flow.

In the Transport of Diluted Species module, the transport of ions is governed by Nernst-Plank equation:

$$J_i = -D_i \nabla n_i + \frac{Z_i e D_i}{KT} n_i E + u \cdot n_i \tag{1}$$

where D_i is the diffusion coefficient of ion type i, n_i is the ionic concentration, Z_i is the valence of ions, e is the elementary charge, K is the Boltzmann constant, T is the temperature, E is the electric field, and u is the fluid velocity. Since the Peclet number is small($Pe << 1$), and so the convective term $(u \cdot n_i)$ can be neglected.

In this model, the Cu cap of the particle surface generates ions at a flux J_i, while the SiO_2 part remains chemically inert. As we assumed the reaction to be first-order, the flux J_i on the Cu surface is defined by:

$$J_i = k_i c_i \tag{2}$$

where c_i is the concentration of the fuel, and k_i is the reaction rate constant.

On the SiO_2 surface, the flux J_i is zero:

$$J_i = 0 \tag{3}$$

In the Electrostatics module, the electric field (E) and electric potential (V) are related by:

$$E = -\nabla V \tag{4}$$

According to Chiang et al.?, the electric field can be obtained by:

$$E = \frac{KT}{e} \frac{\sum_i Z_i D_i \nabla n_i}{\sum_i Z_i^2 D_i n_i} \tag{5}$$

The distribution of the electric field is further governed by the Poisson equation:

$$\nabla \cdot (\varepsilon E) = \rho_v \tag{6}$$

Here, ε is the medium's electrical permittivity, and ρ_v is the space charge density.

In the Creeping Flow module, the fluid velocity (u) and pressure (p) fields satisfy the Stokes flow equations:

$$\nabla \cdot u = 0 \tag{7}$$

$$\nabla p = \eta \nabla^2 u \tag{8}$$

Where η is the dynamic viscosity of water.

As we assumed a thin EDL, the electroosmotic boundary conditions are set at the particle surface:?

$$U_{eo} = \frac{\zeta \varepsilon}{\eta} E_{tan} \tag{9}$$

Here, U_{eo} is the electroosmotic velocity, ζ is the zeta potential of the particle surface, and E_{tan} is the tangential component of the electric field that is obtained from the Equation S5.

For the flow boundary conditions, the top and bottom boundaries of the cylinder are set as open boundaries, while the side walls are set as slip boundaries (no shear stress). Figure S1 provides a schematic representation of the computational setup.

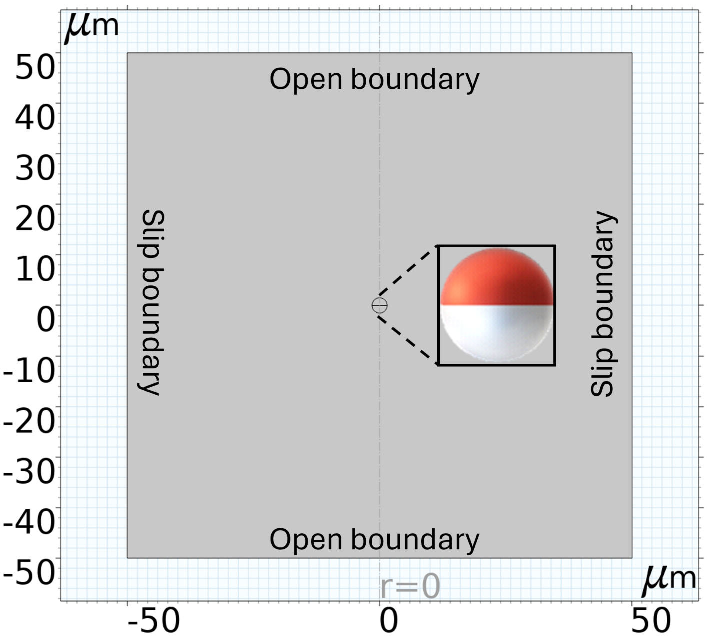

Fig. 1 Schemes of the model used in COMSOL simulations

Since the particle is simulated in its own frame of reference, its actual velocity in the laboratory frame could not be directly extracted. Instead, we use the fluid velocity at the domain edges—where the particle's influence becomes negligible, and a slip boundary condition applies—as a proxy for the particle's translational speed in the laboratory frame, following the approach described by Zhou et al.[9].

Model parameters used in the simulation are as follows:

Table 1 Parameters used in the numerical simulations

Constant	Description	Value
D_{H^+}	Diffusion coefficient of H^+	$9.23\ 10^{-9}\,\mathrm{m}^2/\mathrm{s}$
$D_{\mathrm{Cu}^{2+}}$	Diffusion coefficient of Cu^{2+}	$0.714\ 10^{-9}\,\mathrm{m}^2/\mathrm{s}$
D_{Br^-}	Diffusion coefficient of Br^-	$2.08\ 10^{-9}\,\mathrm{m}^2/\mathrm{s}$
D_{Cu^+}	Diffusion coefficient of Cu^+	$0.73\ 10^{-9}\,\mathrm{m}^2/\mathrm{s}$
D_{I^-}	Diffusion coefficient of I^-	$2.045\ 10^{-9}\,\mathrm{m}^2/\mathrm{s}$
ζ_{Cu}	Zeta potential of the Copper side	-35 mV
ζ_{SiO2}	Zeta potential of the SiO2 side	-40 mV
k_{Br2}	Reaction rate constant of Br2	$3\ 10^{-6}\,\mathrm{m/s}$
k_{I2}	Reaction rate constant of I2	$1\ 10^{-7}\,\mathrm{m/s}$

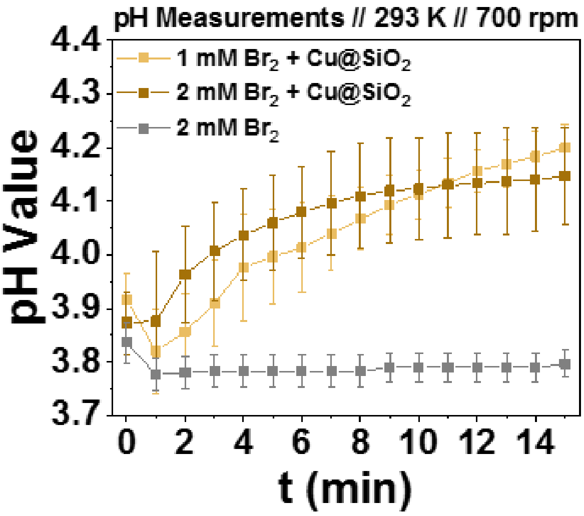

Fig. 2 pH screening over 15 min at room temperature for different concentrations of Br_2 solutions of 1 mM (yellow) and 2 mM (brown), as well as a reference of 2 mM Br_2 solution without an occurred reaction (grey).

The disproportion reaction of Br_2 in water is expected to produce a slightly acidic solution (see Equation 1). If HBrO reacts according to the proposed reaction mechanism, protons should be transferred to water, thereby reducing the solution's acidity (see Equation 2). To investigate this, a simple pH screening was conducted over 15 minutes at room temperature using various concentrations of Br_2 (see Figure S2). Initially, all Br_2 solutions exhibited acidic pH values, as expected. For a 2 mM Br_2 solution where no reaction occurred, the pH remained constant at approximately 3.78. However, when observing the pH evolution in the presence of copper, a significant increase in pH was noted for both the 1 mM and 2 mM Br_2 solutions. In the case of the reaction between 2 mM Br_2 and copper, the pH increased significantly and reached a plateau after approximately 8 minutes. This indicates that the reaction was complete, which is further supported by the absence of visible copper after 6 minutes, confirming that all the copper had been consumed by that point.

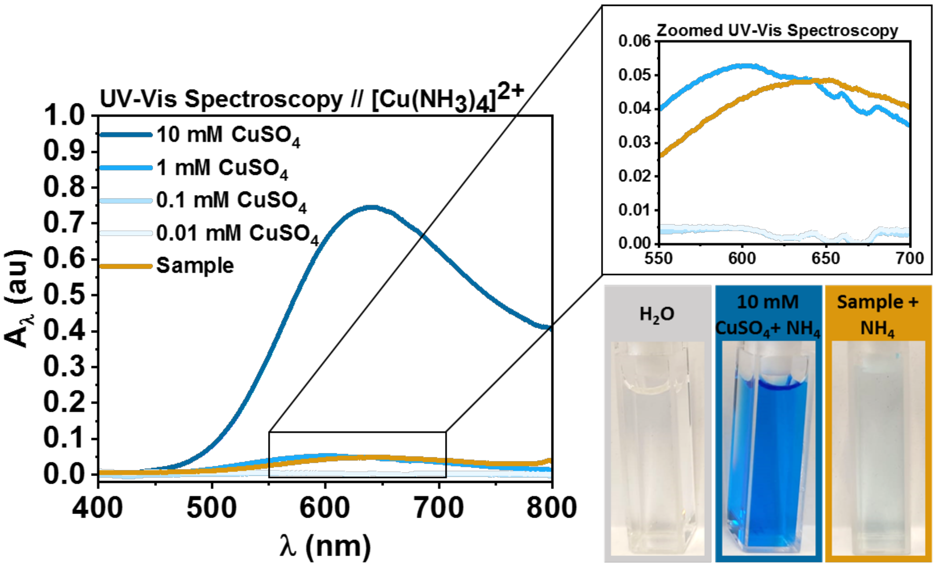

Fig. 3 UV-VIS spectroscopy of $CuSO_4$ solutions at different concentrations (blue shades) and Cu@SiO_2 Janus particles reacted with 666 μM Br_2 fuel (orange), both complexed with NH_3, with sample pictures presented against a white background.

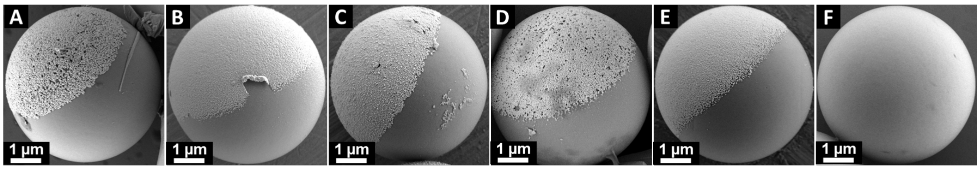

Fig. 4 SEM images of Cu@SiO_2 Janus particles after the reaction with different concentrated Br_2 solutions

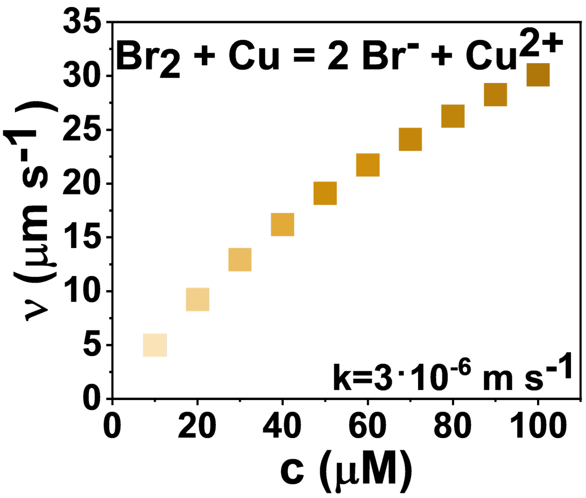

Fig. 5 Simulated Velocities of Cu@SiO_2 Janus particles at different concentrations of Br_2 fuel at a constant reaction rate with no consideration of the disproportion reaction of Br_2 in H_2O.

Figure S5, shows the calculated velocities but without taking the dissociated ions into account, the velocities show a linear increase as the fuel becomes more concentrated resulting in preposterous high calculated velocities. Thus, it is apparent that the ions around the particle have a substantial impact on its velocity, limiting its speed. This interaction between ionic strength and particle swimming speed is already well-known for other systems[?] .

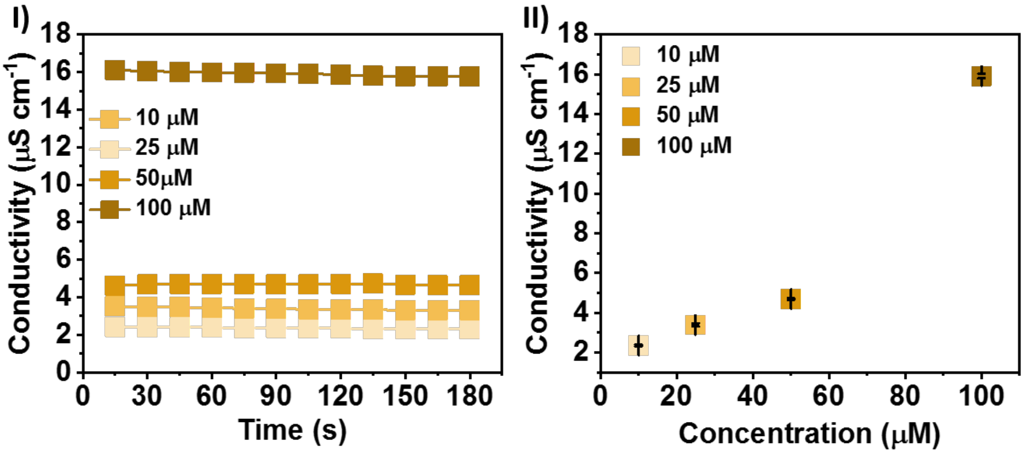

Fig. 6 Measured conductivity of the fuel solutions visualized against I) the time and II) the concentration

The measured conductivity of the Br_2 solution while reacting with Cu@SiO_2 Janus particles is presented in Figure S6. During a reaction time of 3 minutes, no significant change in conductivity is visible. However, it is evident that conductivity generally increases with the concentration of Br_2, as more clearly illustrated in Figure S6 II). This suggests that a higher Br_2 concentration in the solution generates more ions due to its disproportionation in water. Consequently, a higher concentration of the fuel solution leads to more background ions, ultimately affecting the swimming behavior and finally trapping Janus particles at the substrate surface due to the excessive number of background ions.

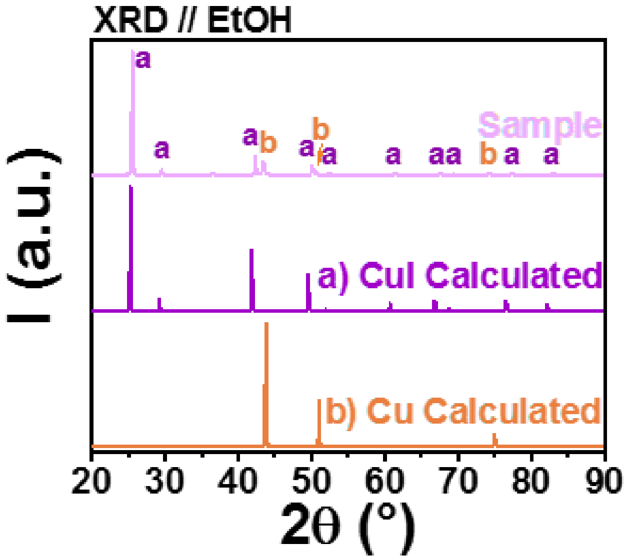

Fig. 7 Calculated XRD diffractogram of Cu (orange) and CuI (purple) and the meassured XRD of the Cu@SiO_2 Janus particle reacted with 500 μM I_2 (pink) from 2θ of 20 to 90 °.

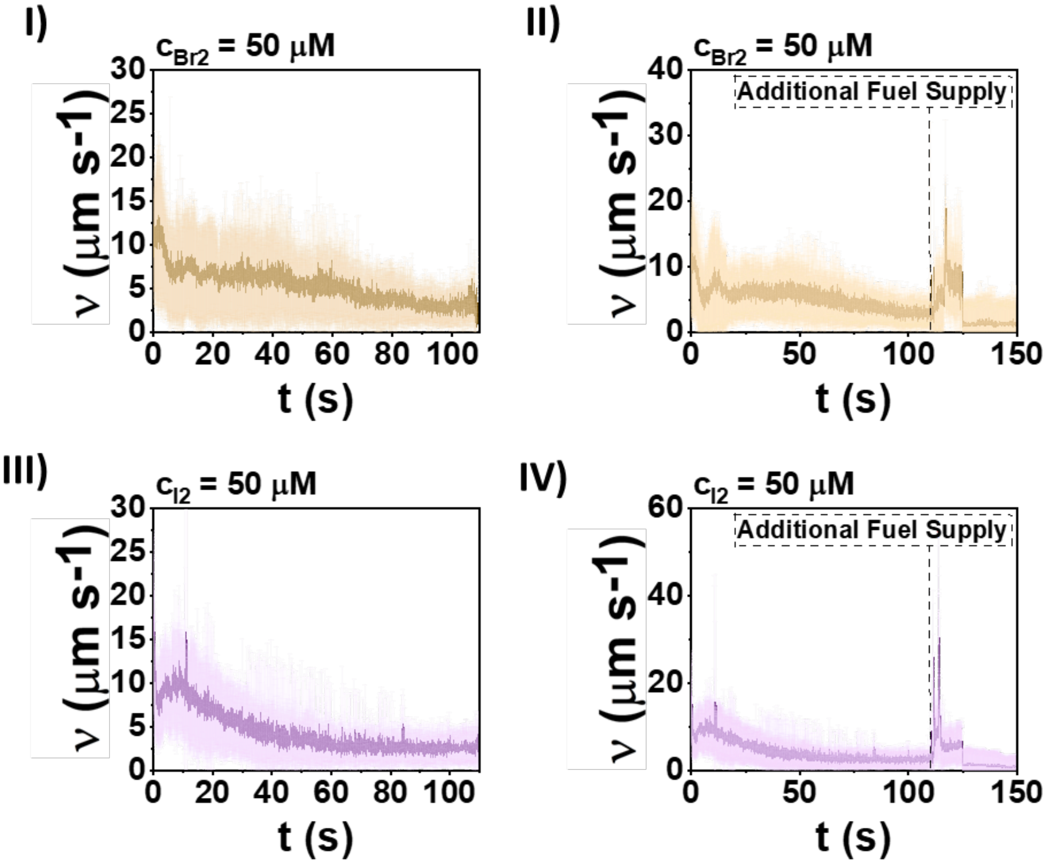

Fig. 8 Swimming Duration of 5 μm SiO2 with a 30 nm Cu cap with I) 50 μM Br_2, II) 50 μM Br_2 with an additional fuel supply after approximately 110 s, III) 50 μM I_2 and IV) 50 μM I_2 with an additional fuel supply after approximately 110 s

The results of swimming duration tests using 50 μM Br2 and I2 fuels are displayed in Figure S8. For Br2 and I2, the velocity development over time is comparable. Bromine allows the particles to swim for at least 20 seconds longer than I2. However, both run for at least a minute and can be restarted with an additional fuel supply, as illustrated in Figures S8 II) and IV). Nevertheless, the extra velocity increase from the second fuel addition is only present for a few seconds.

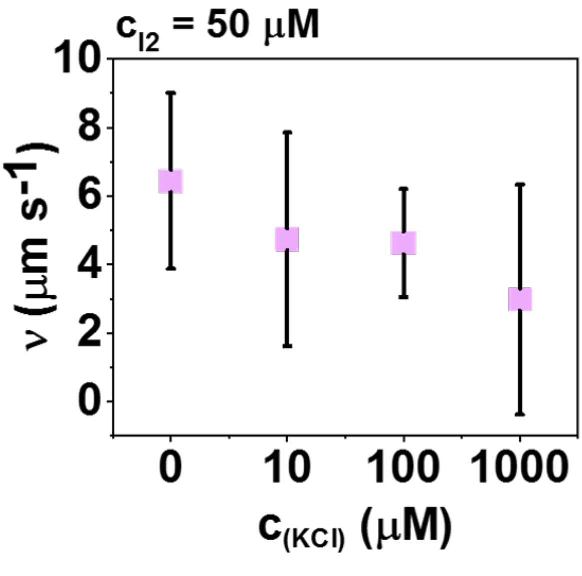

Fig. 9 Influence of increasing background ion concentration (KCl) to the velocity of Cu@SiO_2 Janus particles, propelled by 50 μM I_2

Figure S9 shows how the reactivity of 5 μm SiO_2 particles with a 30 nm half-sided Cu cap in a 50 μM I_2 solution is affected by the introduction of KCl as background ions with increasing concentrations. The obtained mean velocities reveal that while increasing the concentration of background ions, the velocity of Janus particles decreases, but without a monotonic trend. Following Ebbens et al.[?] , this tendency is known for propulsion mechanisms using an ion flow, and it reveals that the propulsion of the Janus particle with I_2 fuel is also powered by electrokinetics.

Supporting Videos

V1: 5 µm Cu@SiO_2 with a 30 nm Cu cap in variyng concentrated Br_2 solutions under the light microscope with 63x magnification

V2: 5 µm Cu@SiO_2 with a 30 nm Cu cap in different concentrated I_2 solutions under the light microscope with 63x magnification

Notes and references

T.-Y. Chiang and D. Velegol, *Journal of colloid and interface science*, 2014, 424, 120–123.

9 C. Zhou, H. Zhang, J. Tang and W. Wang, *Langmuir*, 2018, 34, 3289–3295.

X. Zhan, J. Wang, Z. Xiong, X. Zhang, Y. Zhou, J. Zheng, J. Chen, S.-P. Feng and J. Tang, *Nature communications*, 2019, 10, 3921.

S. Ebbens, D. Gregory, G. Dunderdale, J. Howse, Y. Ibrahim, T. Liverpool and R. Golestanian, *Europhysics Letters*, 2014, 106, 58003.